PROCEEDINGS OF SCIENCE

TAROGE-M: Antarctic High-Mountain Radio Antenna Array for Detecting Ultra-High Energy ANITA Anomalous Events

Shih-Hao Wang[a,b,*] **for the TAROGE and ARIANNA collaborations**

[a] *Department of Physics and Leung Center for Cosmology and Particle Astrophysics, National Taiwan University, No. 1, Sec. 4, Roosevelt Rd., Taipei 10617, Taiwan*

[b] *Institute of Astronomy and Astrophysics, Academia Sinica, Astronomy-Mathematics Building, No. 1, Sec. 4, Roosevelt Rd., Taipei 10617, Taiwan*

E-mail: shwang@asiaa.sinica.edu.tw

TAROGE-M is a radio antenna array atop ~ 2.7 km-high Mt. Melbourne in Antarctica for detecting ultra-high energy (UHE, $E > 10^{17}$ eV) air showers in near-horizontal directions. Besides the detection of cosmic rays and Earth-skimming tau neutrinos, its primary goal is to reproduce the discovery and verify the origin of so-called ANITA anomalous events, having feature of upward-going UHE air showers but cannot be explained by tau neutrinos. The detection concept takes advantages of a high altitude for a broad view toward the horizon; strong and near-vertical geomagnetic field for enhancing the radio signal; and quiet radio environment in Antarctica. Its relatively simple design and high duty cycle make it easily to be extended and thus to achieve an exposure competitive with ANITA experiments within a few years.

The first TAROGE-M station operating at 180–450 MHz frequencies deployed in 2020 detected seven UHE cosmic ray events within 25.3-day livetime. The events have a mean energy of ~ 1 EeV and an estimated flux consistent with other experiments, and validate the station as an UHE particle detector. In 2022–2023 season, the system was upgraded for a robust long-term operation, with a more detailed calibration with a drone-borne pulser. We also discuss the planned upgrade, including the implementation of interferometric trigger, which is expected to increase the cosmic ray and tau neutrino acceptances by a factor of 10 at 0.1 EeV, corresponding to a lower energy threshold by a factor of 3.

38th International Cosmic Ray Conference (ICRC2023)
26 July - 3 August, 2023
Nagoya, Japan

*Speaker

PoS(ICRC2023)1126

1. Introduction

Ultra-high-energy (UHE, over 10^{17} eV) cosmic neutrinos (CNs), charge neutral and weakly interacting, can propagate over cosmological distances without disturbed. They are ideal messengers for resolving long-standing mysteries of UHE cosmic rays (CRs), including their origin and characteristics [1]. Extensive air showers are generated when UHECRs interact with the atmosphere or when UHE tau neutrinos interact with Earth's crust with secondary tau leptons escape and decay into air. The air shower can be efficiently detected by coherent radio pulses it emitted, primarily through the geomagnetic effect that the electrons and positrons in air shower are deflected under the geomagnetic field. The geomagnetic emission is polarized along the Lorentz force direction, with concentrated radiation profile on the Cherenkov ring with $\sim 1^\circ$ opening angle in air [2].

A radio detector at high altitude can observe large volume of Earth's atmosphere and crust as cosmic rays and neutrino targets, respectively, and hence efficient for both UHE cosmic rays and tau neutrinos. The Antarctic balloon-borne experiment ANITA unexpectedly discovered 6 upward-going anomalous air shower events with energies around 1 EeV in its four flights [3**?**]. However, these ANITA anomalous events (AAEs) can not be explained by Earth-skimming tau neutrinos in the Standard Model, because the implied diffuse or transient neutrino fluxes are in tension with the most stringent diffuse flux limits set by IceCube [4] and Auger [5]. Besides, two of AAEs from $\sim$30° below the horizon in which direction the UHE neutrinos are severely attenuated. Unfortunately, the limited live time of the balloon experiment, typically 30 days per flight in 3 years, hinders further significant accumulation of its statistics. Its successor with improved sensitivity, PUEO, is currently in preparation [6].

An alternative approach is to place the radio antenna array at high mountains sensitive to signals in near horizontal directions [7]. Although the detection volume reduces with the altitude, this approach has advantages of lower energy threshold, higher duty cycle, and easier to scale up. Thus, a high-mountain radio detector offers greater potential, in principle, to achieve similar sensitivity as ANITA's and beyond, expediting the verification process of the origin of AAEs. Similar ideas were also proposed by BEACON [8] and GRAND [9]. In particular, Antarctic mountains are ideal places for this method, not only for its low radio-frequency (RF) background, but also for its strong (>60 μT) and nearly vertical geomagnetic field almost perpendicular to near horizontal showers which maximizes the strength of signal primarily in horizontal polarization.

Therefore, we built the first antenna station in 2020 [10] atop Mt. Melbourne (74°20′55.88″ S, 164°41′35.38″ E), a 2720 m high Antarctic volcano, accessible by helicopter and $\sim$30 km away from Korean Jang Bogo station (JBS) providing logistic support. Using tau neutrinos as a proxy of AAEs, simulation shows that a single TAROGE-M station with half year of operation is expected to have a comparable sensitivity as ANITA's [10]. This paper summarizes the result of UHECR detection in TAROGE-M data in 2020, formerly published in Ref. [10]. In addition, the upgrade and the status of TAROGE-M in 2023 are presented.

2. Upgraded Design of TAROGE-M in 2023

The design of the first TAROGE-M station deployed in 2020 is detailed in Ref. [10]. Several upgrades had been made since then and the station was redeployed in Feb 6, 2023. Eight new

Figure 1: TAROGE-M station redeployed on the top of Mt. Melbourne in Antarctica in Feb 2023.

log-periodic dipole antennas (LPDAs, previously six) of 7 dBi gain at 180–800 MHz comprise the receivers of upgraded TAROGE-M station, and they have reinforced structures for withstanding the high wind (up to 50 m/s). For the polarimetry, six of LPDAs are horizontally polarized (Hpol) to align with the geomagnetic emission, and two of them are vertically polarized (Vpol). Seven of LPDAs point to toward northern horizon, whereas one Hpol points to opposite direction for vetoing potential RF interference (RFI) behind the station. LPDAs are mounted on 3 m high towers, with 8–11 m separation for reconstructing the signal direction based on their time difference of arrivals (TDOAs), as shown in Fig. 1. Each antenna is connected with a 15 m coaxial cable to the RF front-end module of overall 58 dB gain, consisting of 180–450 MHz band-pass filter, 340–380 MHz band-stop filter, and low-noise amplifiers.

For the data acquisition (DAQ), received signals are processed by an 8-channel SST board originally designed for the ARIANNA neutrino experiment at Ross Ice Shelf and South Pole [11]. The signal of each channel is sampled and digitized with 1 GHz rate and 12-bit resolution, and 256 samples are saved upon trigger. The level-0 (L0) trigger is formed by two stages. First, a channel-level trigger requires that the received waveform exceeds both positive and negative thresholds within 5 ns window for 5 Hpol channels, where the threshold was set between ±3.5 to ±4 times the RMS noise voltage (typically 16 mV). Then a station-level one requires 3- or 4- out-of-5 Hpol coincidence triggers within 75 ns (previously 3 out of 4 Hpols in 32 ns). The longer window makes all 5 Hpol channels (instead of 3 closer ones in 2020) able to form trigger for inclined showers. The successive level-1 (L1) trigger rejects narrow-band noise by computing the ratio of the peak magnitude of amplitude spectrum to the remaining sum. In addition, forced trigger of 100 s period was configured for monitoring the RF background and the health of receivers.

As only partial data can be transferred out via Inmarsat satellite communication of limited data bandwidth, the recorded events are further filtered online by a single-board computer for selecting Hpol impulsive events, based on the spectral analysis (see Sec. 5) which retains 99.9% efficiency to CR signals. The full data is stored locally in an SD flash memory card.

The hybrid power module consists of twelve 30 W solar panels and 150 Ah absorbent glass mat batteries to support full-time operation throughout austral summer from August to April, and a 10 W wind turbine (at 12 m/s wind speed) for testing extended operation in winter (May to July). The module has been modified to resolve the power problems in 2020, and is more robust at low temperatures. All active electronic devices are contained inside a stainless steel box for shielding self-generated RFI, and the box is inside a thermally insulated weatherproofing enclosure

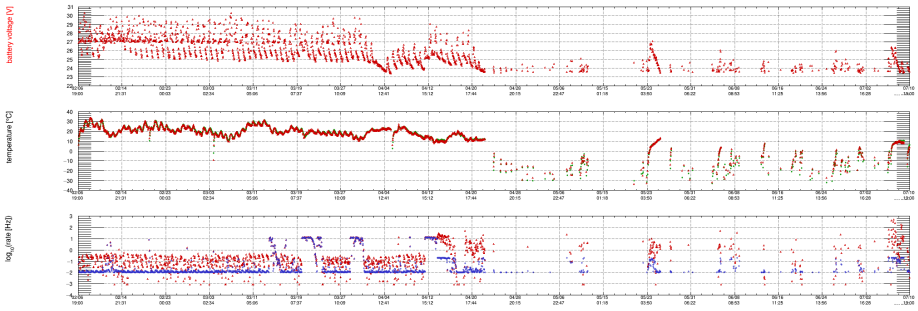

Figure 2: TAROGE-M operation summary in 2023 since its deployment at Feb 6 until Jul 10. The horizontal time axis in UTC, and the polar night starts at May 6. Top: Battery voltage of 24 V solar and wind hybrid power system. Middle: Temperature measured by SST board (green) and power board (red) inside weatherproofing enclosure. Bottom: Event rate in logarithmic scale, with red dots indicating the L0 trigger and blue for L1 trigger plus 0.01 Hz forced trigger.

maintaining the internal temperature ~40 °C higher than the ambient temperature (down to −50 °C in winter) during the operation.

3. Operation Summary in 2023

TAROGE-M in 2023 has overcome the power problem resulting in premature operation interruption with only 26.5-day live time in 2020. The station has continuously operated until early April since its redeployment at Feb 6, 2023, as shown in Fig. 2.[1] The system has near 100 % duty cycle with the solar power, indicated by the daily variation of battery voltage and internal temperature in Fig. 2, until April 23 when the daytime becomes less than 6 hours per day. After local polar winter started from May 6, TAROGE-M still has intermittent operation, with an uptime of ~9 days over 61 days. proving the wind power prototype worked properly. As of the date of writing (July 11), TAROGE-M station has been accumulating data with ~ 77-day live time in 2023.

The typical event rate after L1 trigger is 10^{-2}–10^{-3} Hz, but there were episodes of high event rate at 1–10 Hz with predominant impulsive noise, as shown in Fig. 2, similar as previously reported in 2020 [10]. The episodes are correlated with high wind speed (>7 m/s), and similar phenomenon has also been reported by other polar radio experiments. The noise is likely generated by the triboelectric effect between blown ice crystals and metallic objects (see Ref. [12] for a detailed review). These high-wind events are the main noise source for TAROGE-M, accounting for > 99% of recorded events, and thus they have to be effectively rejected in the analysis. To prevent high-wind events consuming all the data storage, an upper limit of the L1 event rate at 0.2 Hz was set in triggering since Apr 14 (the blue step at bottom panel of Fig. 2). Despite struck by several storms, the noise power of forced-trigger events shows the radio receivers are still in good shape.

Initial one month of data was retrieved at the last site visit for drone flights, and full data will be available in next season after retrieving the SD card from TAROGE-M. In summary, the TAROGE-M has successfully conducted long-term operation and demonstrates the feasibility of extended operation in polar night.

[1] except two manual shutdowns for replacing SD card to retrieve full calibration pulser data, indicated by low temperature at system reboot during February and March.

4. In-Situ Calibration

To reliably reconstruct the source direction of a radio signal and thus distinguish downward-going CR from upward-going AAEs and neutrinos based on TDOAs between antennas, it is critical to accurately calibrate the position and the timing of each receiver. Besides, the receiver response needs to be calibrated for accurately reconstructing the electric field and hence the primary energy of air-shower signal. The in-situ calibration procedures for TAROGE-M 2023 follows those in 2020 [10] with several improvements.

The photogrammetry was used for a fast survey of the antenna station in the field, together with the differential GPS (DGPS) module of drone-borne pulser providing accurate reference points [13]. The resulting station model has an improved accuracy in both antenna positioning and orientation, better than 1 mm and 0.1°, respectively. For calibrating the receiver gain, the noise power of forced-trigger events at 180–240 MHz were used The power varies periodically in a sidereal day and is consistent with that of the Galactic noise. The gain calibration with the Galactic noise was shown to have ∼5 % precision in 2020 data [10].

4.1 Drone-Borne and Ground-Based Calibration Pulser

A drone-borne calibration pulser system was developed in 2020 for calibrating the event reconstruction in near horizontal directions which is difficult to access by other means. The drone pulser has characterized the trigger efficiency and the angular resolution of TAROGE-M, with 0.2° in azimuth and 0.3° in zenith angles [10]. The system, consisting of a DGPS module with centimeter-level positioning and a pulser module configurable in the field, has been improved in 2023, as detailed in Ref. [13]. The flight plan was also improved. Three drone flights were completed on Mar 4, 2023, scanning a denser angular grid and extended to below the horizon at ∼500 m distance to the station, spanning azimuth angle $\phi = [-50°, 50°]$ (0° at the geographic North) and zenith angle $\theta = [77.5°, 92.5°]$. The pulser was set to 9 Hz pulsing rate for higher statistics and varying strength over 18 dB power dynamic range for measuring the trigger efficiency. Roughly 9000 pulser events were detected. One main purpose is to understand the differential interference of reflected signals off the ground (permafrost) on different antennas, which effect becomes more significant for events in near horizontal directions.

In addition, a new ground-based calibration pulser system was developed and deployed at Baker Rocks 13 km away from Mt. Melbourne and is −8.6° below the horizon from TAROGE-M. The pulser system was active from Feb 15 to Mar 13, regularly transmitting five pulses of different amplitudes at every hour, providing long-term monitoring of event reconstruction performance, complementary to the drone-borne pulser. The calibration analysis is currently in progress.

5. Ultra-High Energy Cosmic Ray Detection in 2020 Data

An analysis searching for UHECR events in 26.5-day data in 2020 was performed to demonstrate TAROGE-M is able to detect UHE air showers, and 7 UHECR events were identified. This section summarizes the procedures and result detailed in Ref. [10].

The UHECR detection simulation of TAROGE-M incorporates and CoREAS [14] for expected radio electric fields, with 992 proton-initiated air showers generated with primary energies spanning

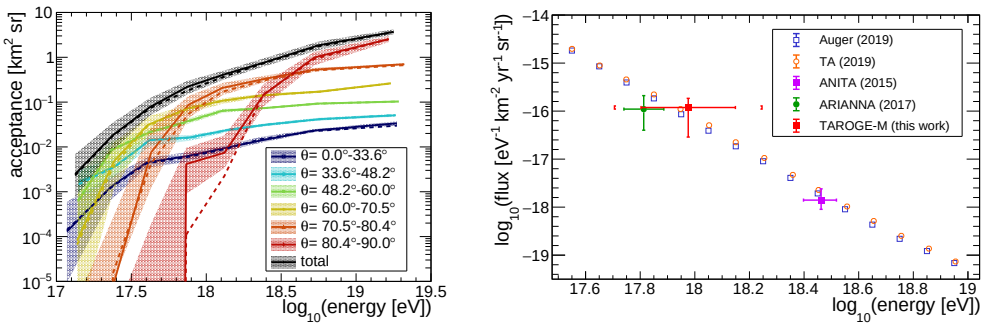

Figure 3: Left: Expected cosmic ray acceptance as a function of primary energy for TAROGE-M in 2020, each color for a zenithal range. Solid (dashed) curves are the result with (without) the reflected signal from the ground, with shaded area for the uncertainty. Right: Measured cosmic ray flux by TAROGE-M in 2020 (red square), versus those by Auger [15], TA [16], ANITA [17], and ARIANNA [11]. Figures from Ref. [10].

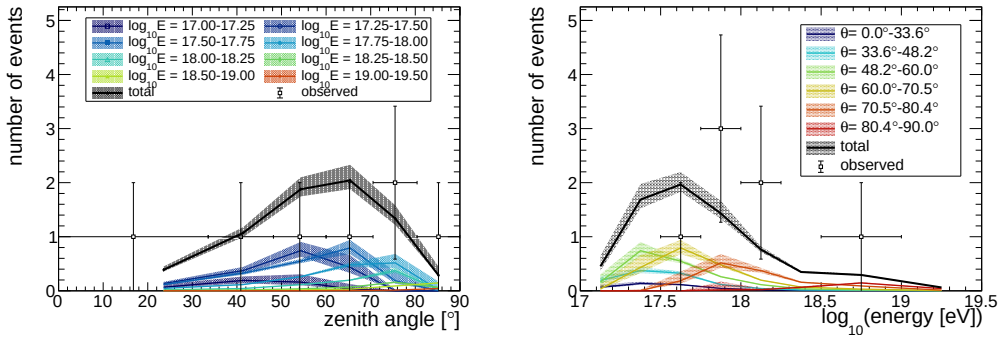

Figure 4: The zenith-angle (left) and energy (right) distributions of seven detected UHECR events in TAROGE-M 2020 data (black circles), compared with the simulated results assuming Auger cosmic ray spectrum [15] (colored curves, scaled to the number of observed events). Figures from Ref. [10].

0.1–30 EeV and directions in front of the station. The received field has an extra component from reflection off the ground and was convolved with the receiver response, and them processed by a trigger simulation of SST board. The resulting cosmic ray acceptance as a function of primary energy is shown in Fig. 3, and expected event distributions shown in Fig. 4.

There are 1, 257, 122 recorded RF-trigger events within 26.5-day live time in 2020. Unlike the air shower signal primarily Hpol with a falling broadband spectrum with frequency, the predominant impulsive high-wind noise have a particularly high amplitude only at one of channels than the others, and are also preferably from behind the station likely from metallic objects of nearby facilities. Thus, the noise can be effectively rejected by these two features, based on a spectral analysis using power within the signal band defined at 180–240 MHz and 280–330 MHz. Only 319 events passed these two criteria, with a CR signal efficiency of 99.9%.

Other common noise and its rejection method include: the satellite communication noise, rejected by the band power at 240–280 MHz; Vpol-dominated anthropogenic noise, rejected by Hpol-to-Vpol power ratio; random thermal noise, rejected by the quality of event reconstruction based on interferometric technique [10]. The selection thresholds were driven by forced trigger

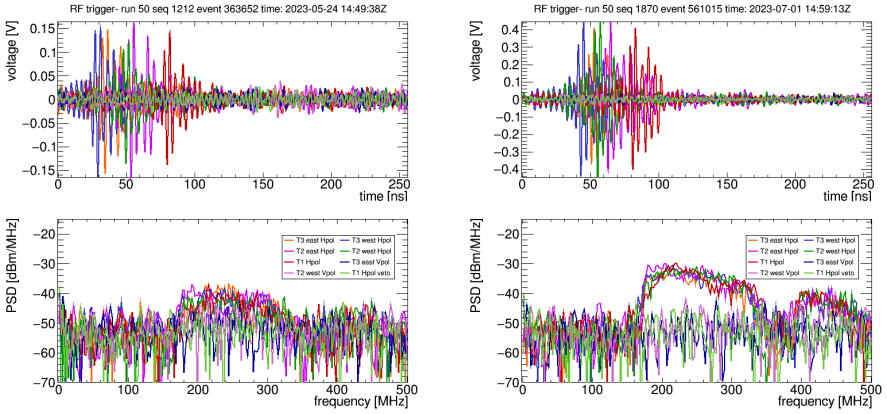

Figure 5: Waveforms (top) and spectra (bottom) of two UHECR candidates detected during polar night in 2023. The left one is from $(\theta, \phi) = (79.5°, -2.8°)$ and the right from $(\theta, \phi) = (59.7°, 3.9°)$.

events to avoid systematic uncertainty from the simulation and keep weak signals. Lastly, temporal isolation is required on remaining events that there should be no more than one event within a time window of ±600 seconds, as air shower signals are expected to be rarer.

After all selection criteria were applied, 7 UHECR events were identified in 25.3-day data, [2] with 90% CR signal efficiency, and are consistent with the expected number of $4.4^{+0.3}_{-0.2}$. All of the events have polarization consistent with the geomagnetic emission. The primary energy of each event was measured by fitting the logarithmic amplitude spectrum with a linear function, following the same method used in ANITA and ARIANNA [10, 11, 17]. The UHECR events have zenith angles between 25° to 82°, with mean reconstructed energy of $0.95^{+0.46}_{-0.31}$ EeV. Both the zenithal and energy distributions are consistent with the simulations, as shown in Fig. 4. The corresponding cosmic ray flux at the energy, $1.2^{+0.7}_{-0.9} \times 10^{-16}$ eV^{-1} km^{-2} yr^{-1} sr^{-1}, is also consistent with previous results of other experiments, as shown in Fig. 3. Therefore, we verified TAROGE-M's discovery potential of detecting UHE air showers.

6. Preliminary Result of TAROGE-M 2023

Among the events selected by online filtering, 22 UHECR candidate events have been identified in 77-day live time, including three detected during polar night, two of them shown in Fig. 5. The corresponding event rate is ∼ 1.7 times higher than that in 2020 mainly because of a longer coincidence trigger window described in Sec. 2. In addition, there are several impulsive events in a similar direction from below the horizon and features as those three successive ones of unknown origin discovered in 2020 data passing all selections except the temporal isolation [10]. we later realized that their directions roughly coincide with the autonomous seismic stations in field of view, and further analysis on these events is ongoing.

[2] 1.2 days out of 26.5-day data were excluded for characterizing high wind noise.

7. Conclusion and Prospects

The TAROGE-M's ability to detect UHE air showers has been verified by the seven detected UHECR events in 2020, showing its discovery potential of AAEs. Its long-term operation extending to polar night and reliability in polar and high-altitude environment are also verified with the upgraded system in 2023. With proper scale-up of the wind power system in next season, a duty cycle of 10-month operation annually or higher can be expected. The interferometric trigger is currently under development with the RF system-on-chip (RFSoC) technology to increase the sensitivity in near horizontal directions. Simulation suggests implementing the interferometric trigger to current system will increase the cosmic ray and tau neutrino acceptances by a factor of 10 at 0.1 EeV, corresponding to a lower energy threshold by a factor of 3. The front-end modules will be modified and directly connected with the antennas to reduce the effective receiver temperature. More stations will be deployed at different locations of Mt. Melbourne in next couple of years. We hope further observation and expansion of TAROGE-M can help to expedite the verification of the origin of ANITA's anomalous events.

References

[1] M. Ackermann et al., *Journal of High Energy Astrophysics* **36** (2022) 55.

[2] F.G. Schröder, *Progress in Particle and Nuclear Physics* **93** (2017) 1.

[3] ANITA collaboration, *Phys. Rev. Lett.* **121** (2018) 161102.

[4] IceCube collaboration, *The Astrophysical Journal* **892** (2020) 53.

[5] ANITA collaboration, *Phys. Rev. D* **105** (2022) 042001.

[6] Q. Abarr et al., *Journal of Instrumentation* **16** (2021) P08035.

[7] J. Nam et al., *PoS* **ICRC2019** (2020) 967.

[8] BEACON collaboration, *Nucl. Instrum. Methods Phys. Res., Sect. A* **1048** (2023) 167889.

[9] GRAND collaboration, *Sci. China Phys. Mech. Astron.* **63** (2020) 219501 [1810.09994].

[10] TAROGE and ARIANNA collaboration, *JCAP* **2022** (2022) 022.

[11] ARIANNA collaboration, *Astroparticle Physics* **90** (2017) 50.

[12] J. Aguilar et al., *Astroparticle Physics* **145** (2023) 102790.

[13] C.-Y. Kuo et al., *PoS* **ICRC2023** (2023) 512.

[14] T. Huege, M. Ludwig and C.W. James, *AIP Conference Proceedings* **1535** (2013) 128.

[15] V. Verzi et al., *PoS* **ICRC2019** (2019) 450.

[16] D. Ivanov et al., *PoS* **ICRC2019** (2019) 298.

[17] H. Schoorlemmer et al., *Astroparticle Physics* **77** (2016) 32.

Acknowledgements

We wish to thank the supports from National Science and Technology Council (NSTC) for the TAROGE-M project under grant 111-2112-M-002-034, and from Korea Polar Research Institute (KOPRI), and the great logistics and field support from on-ice Jang Bogo station crews in 2018–2019, 2019–2020, and 2022–2023 seasons. We would like to acknowledge support from the Taiwan Ministry of Science and Technology (MOST) for the TAROGE-M project under grant 110-2112-M-002-037.This work was also partly supported by research grant PE22020 from KOPRI. We are grateful to the U.S. National Science Foundation-Office of Polar Programs, the U.S. National Science Foundation-Physics Division (grant NSF-1607719) for supporting the ARIANNA array at Moore's Bay, and NSF grant NRT 1633631 and Award ID 2019597. We acknowledge funding from the German research foundation (DFG) under grants NE 2031/2-1, and the Swedish Government strategic program Stand Up for Energy.

Full Authors List:

TAROGE Collaboration

Pisin Chen[1,2,3], Yaocheng Chen[1,2], Ying-Chih Chen[1,2], Taejin Choi[4], Young-bae Ham[4,5], Shih-Ying Hsu[1], Jian-Jung Huang[1,2], Ming-Huey A. Huang[6], Geonhwa Jee[4,5], Jongil Jung[7], Jieun Kim[4], Chung-Yun Kuo[1,2], Hyuck-Jin Kwon[4], Changsup Lee[4,5], Chung-Hei Leung[1,2,8], Tsung-Che Liu[1,9,10,11,12], Jiwoo Nam[1,2], Yu-Shao J. Shiao[2,13] Bok-Kyun Shin[2,14], Shih-Chieh Su,[1,2], Min-Zu Wang[1,2], Shih-Hao Wang[1,2,15], Yu-Hsin Wang[1,2]

[1] Department of Physics, National Taiwan University, Taipei 10617, Taiwan
[2] Leung Center for Cosmology and Particle Astrophysics, National Taiwan University, Taipei 10617, Taiwan
[3] Kavli Institute for Particle Astrophysics and Cosmology, SLAC National Accelerator Laboratory, Stanford University, Stanford, CA 94305, USA
[4] Division of Atmospheric Sciences, Korea Polar Research Institute, Incheon, Republic of Korea
[5] Department of Polar Science, Korea University of Science and Technology, Daejeon, Republic of Korea
[6] Department of Energy Engineering, National United University, Miaoli, Taiwan
[7] Department of Astronomy, Space Science and Geology, Chungnam National University, Daejeon 34134, Republic of Korea
[8] Department of Physics and Astronomy, University of Delaware, Newark, DE 19716, USA
[9] Department of Electrophysics, National Yang Ming Chiao Tung University, Hsinchu 300, Taiwan
[10] Department of applied physics, National Pingtung university, Pingtung 900, Taiwan
[11] Chung Cheng Institute of Technology, National Defense University, Taoyuan 335, Taiwan
[12] Undergraduate Degree Program of Systems Engineering and Technology, National Yang Ming Chiao Tung University, Hsinchu 300, Taiwan
[13] National Nano Device Laboratories, Hsinchu 300, Taiwan
[14] Ulsan National Institute of Science and Technology, Ulsan 44919, Republic of Korea
[15] Institute of Astronomy and Astrophysics, Academia Sinica, Astronomy-Mathematics Building, No. 1, Sec. 4, Roosevelt Rd., Taipei 10617, Taiwan

ARIANNA Collaboration

Astrid Anker[1], Steven W. Barwick[1], Dave Z. Besson[2], Sjoerd Bouma[3,4], Maddalena Cataldo[4], Geoffrey Gaswint[1], Christian Glaser[5], Steffen Hallmann[3], Jordan C. Hanson[6], Jakob Henrichs[3,4], Stuart A. Kleinfelder[7], Robert Lahmann[4], Zachary S. Meyers[3,4], Anna Nelles[3,4], Alexander Novikov[2], Manuel P. Paul[1], Lilly Pyras[3,4], Christopher Persichilli[1], Ilse Plaisier[3,4], Ryan Rice-Smith[1], Mohammad F.H. Seikh[2], Joulien Tatar[8], Christoph Welling[3,4], Leshan Zhao[1]

[1] Department of Physics and Astronomy, University of California, Irvine, CA 92697, USA
[2] Department of Physics and Astronomy, University of Kansas, Lawrence, KS 66045, USA
[3] DESY, 15738 Zeuthen, Germany
[4] ECAP, Friedrich-Alexander-Universität Erlangen-Nürnberg, 91058 Erlangen, Germany
[5] Uppsala University Department of Physics and Astronomy, Uppsala SE-752 37, Sweden

[6] Whittier College Department of Physics, Whittier, CA 90602, USA
[7] Department of Electrical Engineering and Computer Science, University of California, Irvine, CA 92697, USA
[8] Research Cyberinfrastructure Center, University of California, Irvine, CA 92697, USA